Terra Nova

WILEY

Terra Nova

RESEARCH ARTICLE OPEN ACCESS

Emergence of Continents Stabilized the Bioavailability of Boron

Brendan V. Dyck[1] | Jon Wade[2]

[1]Department of Earth & Environmental Sciences, University of British Columbia, Kelowna, British Columbia, Canada | [2]Department of Earth Sciences, University of Oxford, Oxford, UK

Correspondence: Brendan V. Dyck (brendan.dyck@ubc.ca)

Received: 19 November 2025 | **Revised:** 31 March 2026 | **Accepted:** 5 April 2026

Keywords: boron | EBSD | element cycles | epitaxy | nucleation | RNA world | tourmaline

ABSTRACT

Boron is an essential element for the development of life on Earth; borates stabilize ribose in prebiotic reactions and facilitate metabolism in higher plants. There is, however, a relatively narrow surface boron concentration range over which borates stabilize and serve as a micronutrient rather than a toxin. That life evolved to utilize borates suggests that the boron concentration in surface waters must have remained relatively stable over much of Earth's history. Here we show that natural tourmaline nucleation is facilitated by epitaxy on the mica minerals; common constituents of peraluminous continental crust. By reducing the kinetic barrier to tourmaline nucleation, epitaxy has helped to enable the long-term sequestration of boron within Earth's continents and has helped maintain a stable abundance of bioavailable boron going back at least ca. 3.7 Ga.

The distribution of the bulk Earth's boron inventory is a consequence of boron's high solubility in water and volatility. Outgassing of Earth's primitive mantle in the first ca. 100 Ma of the Earth's history (Ballentine and Holland 2008; Rubey 1951) led to a significant portion (> 60%) of Earth's boron being concentrated in the hydrosphere. Consequently, the transport of boron has since been inextricably linked to the global water cycle, which includes magmatic and hydrothermal processes and, after the onset of plate tectonics, the recycling of oceanic lithosphere (Marschall 2018). Like chlorine, boron is highly soluble in both water and silicate melt and promotes chemical differentiation of continental crust by lowering the solidus of silicate-melt (London 2011; Thomas et al. 2023). Whereas ~95% of Earth's chlorine is held in its oceans (Schilling et al. 1978), approximately one third of Earth's boron resides in the continental crust, bound in the crystal structures of the tourmaline-group minerals (Grew 2017; Henry et al. 2011).

The bulk Earth's boron content is only loosely constrained at $\sim 1 \times 10^{18}$ kg (Sun and McDonough 1989)—a consequence of its moderate volatility during terrestrial accretion (Wood et al. 2019) and the possibility that it is mildly siderophile during core formation (Yuan and Steinle-Neumann 2022). The undepleted mantle is thought to be the largest reservoir for terrestrial boron, containing approximately one third of Earth's total boron (38% ± 4%), followed closely by continental crust (30% ± 5%) and depleted mantle (25% ± 3%) with oceans accounting for considerably less (0.83% ± 2%) at approximately 10^{15} kg B (Marschall et al. 2017). The average boron concentration of the continental crust is 17 μg/g B (Rudnick and Gao 2003). In contrast, the present-day upper mantle is depleted in boron such that modern mid-oceanic ridge basalts exhibit ~1 μg/g B (Chaussidon and Jambon 1994; Marschall et al. 2017).

1 | Earth's Boron Cycle

Earth's surface inventory of boron has been effectively buffered by its exchange between the continents and the hydrosphere over geologic timescales. Chemical weathering and hydrothermal remobilization of boron from crustal sources, principally granites (213–287 μg/g B) and terrigenous sediment (30–150 μg/g

B), adds boron to surface reservoirs (Leeman and Sisson 1996). Boron is removed from the hydrosphere via seawater alteration of oceanic crust and adsorption to terrigenous clays on the seafloor where it resides until it is recycled at convergent margins (Marschall 2018). At ocean–ocean and ocean–continent margins, expulsion of pore fluids at the onset of subduction only returns ~10% of the ocean-exchangeable boron (You et al. 1993). The remaining ~90% of boron is released during metamorphic dehydration of the ocean slab and overlying sediments, where it enters fore-arc and volcanic arc systems and rises toward the surface as a component of silicate melt and aqueous fluid. At Himalayan-style continent–continent margins, boron hosted in (aluminium-rich) terrigenous sediments is retained during prograde metamorphism and is subsequently sequestered as metamorphic tourmaline within orogenic belts. The retention of boron in metamorphosed terrigenous sediments results from its incorporation into peraluminous phyllosilicates and tourmaline, minerals that are stable in aluminium-rich lithologies across a wide range of metamorphic conditions (Palin and Dyck 2021; Van Hinsberg et al. 2011). While some slab and sediment-derived boron may bypass the crustal reservoir, leading to the elevated levels of boron in volcanic derived groundwaters, the majority is instead held within the continental crust (and volcanic arcs) by minerals of the tourmaline supergroup, the most abundant species of which being schorl and dravite $Na(Fe^{2+}, Mg)_3Al_6(Si_6O_{18})(BO_3)_3(OH)_3(OH)$ (Henry et al. 2011). Although evaporites can also be enriched in borates, they constitute only a minor fraction of the continental crust (Garrett 1996). Given that granitic rocks comprise ~25%–40% of the continental crust whereas sedimentary rocks account for $<10\%$ of the continental crust and only a small subset of these are evaporites (Touret et al. 2022; Wedepohl 1995), it is reasonable to infer that the majority of continental boron is hosted in tourmaline rather than borates.

2 | Hindered Homogeneous Nucleation of Tourmaline

Experimental studies show that tourmaline exhibits delayed or incomplete homogeneous nucleation in crustal melting experiments (Scaillet et al. 1995; Wolf and London 1997), a consequence of its large and complex acentric rhombohedral crystal structure. In these experiments, tourmaline instead forms via reaction with ferromagnesian aluminosilicate-minerals such as the mica group minerals biotite and chlorite (London 1999). As such, the determination of tourmaline stability has largely relied on experiments seeded with crystals of tourmaline compositions that remain crystalline throughout the melt-present stage of the experiments (London 2011; Vorbach 1989). In natural diagenetic environments, tourmaline similarly preferentially nucleates on fragments of detrital tourmaline (Henry and Dutrow 1996). Natural magmatic tourmaline also exhibits microstructural evidence for hindered nucleation with a tendency toward stellate radial growth, as well as forming large, yet few, crystals (Byerly and Palmer 1991; London 2011). While there are no experimentally derived estimates for the activation energy of homogeneous tourmaline nucleation, reported values from the structurally similar aluminosilicate phases m-cordierite and a-cordierite are relatively large, ranging between 532–574 and 399–426 kJ mol^{-1} (Donald 1995). If natural tourmaline is similarly hindered in its nucleation, as is indicated by the experimental data and observations of crystal microstructures, or if the magmatic-hydrothermal system does not evolve to form peraluminous rocks, the implication is that boron sequestered in ocean-floor deposits is efficiently returned to surface waters at convergent plate boundaries. Yet, despite the overwhelming experimental evidence for its hindered nucleation, tourmaline within the continental crust hosts a significant portion of Earth's boron inventory. Although seemingly peripheral, the mechanisms of natural tourmaline nucleation are therefore key to understanding the secular evolution of the Earth's boron cycle.

3 | Epitaxial Nucleation of Tourmaline on Biotite and Chlorite

Natural tourmaline is often strongly associated with the mica-group minerals biotite and chlorite which are the primary ferromagnesian peraluminous phases in the granite and metasedimentary rocks that comprise most of Earth's upper continental crust (Rudnick and Gao 2003). Intergrowths of tourmaline–biotite and tourmaline–chlorite are present in orogenic belts and volcanic arcs throughout the rock record, with earliest examples found in the ca. 3.7 Ga Isua greenstone belt in Greenland (Grew et al. 2015). The microstructure of tourmaline-mica intergrowths—commonly described as comb microstructures—are consistent with preferred nucleation of tourmaline on the mica (001) cleavage planes (Dyck and Larson 2023).

To demonstrate the natural nucleation tendencies of incipient tourmaline growth, we took examples that span the majority of Earth's history; including Cenozoic (ca. 18 Ma) tourmalines from the intrusive margins of Himalayan granites in the Langtang valley, Nepal and tourmaline grown along chlorite (001) planes in samples from the Eoarchaean (ca. 3700 Ma) Isua Greenstone Belt, Greenland. We applied electron backscatter diffraction to identify the neighbour-pair tourmaline–biotite and tourmaline–chlorite orientation relationships. Figure 1A,B summarizes our findings of ubiquitous epitaxy in both mineral pairs, a relationship that is characterized as the {10–10} planes of tourmaline parallel to mica (001) with the tourmaline *c*-axes [0001] parallel to the mica [010] directions. Mechanistically, this epitaxial relationship is consistent with tourmaline nuclei having been aligned by the electrostatic attraction of its cations (Fe, Mg, Al, Na) with the apical oxygen of the silica tetrahedral exposed along the perfect cleavage planes (001) of both micas (Figure 1C–E).

The activation energy required to epitaxially nucleate a phase on a planar substrate is lower than that of homogeneous nucleation and equal to the product of homogeneous nucleation and a function of the contact angle (Θ) (Kelton 2001)

$$\Delta G_{\text{heterogeneous}} = \Delta G_{\text{homogeneous}} \cdot f(\theta), \text{where } f(\theta) = \frac{2 - \cos\theta + \cos^3\theta}{4}.$$

Classical nucleation theory assumes nucleation from a homogeneous, isotropic medium and equilibrium interfacial energies between phases; these assumptions are only approximations when applied to complex, chemically heterogeneous silicate systems where anisotropic crystal structures,

compositional variability and fluid–solid interactions may influence nucleation behaviour (Markov and Stoyanov 1987). Nevertheless, this framework provides a useful first-order means of evaluating the relative energetic advantage of heterogeneous nucleation in natural mineral assemblages. To quantify the contact (dihedral) angle associated with tourmaline epitaxy, we measured the contact angles (θ) of triple junctions formed by tourmaline–biotite (001)–quartz using a polarized light microscope with a universal stage. For the contact angle measurements, we focus on the samples from the Langtang Himalaya because they represent an incipient fluid-saturated reaction front (Dyck and Larson 2023) that did not experience any subsequent thermal metamorphism that could have modified the primary contact angles. The measured angles are bimodally distributed with median and standard deviation angles for the two modes of 32° ± 18° ($n = 34$) and 146° ± 19° ($n = 37$) (Figure 2). The low-angle mode is associated with the primary wetting properties of tourmaline on biotite (001) in a matrix of quartz (Figure 2A), whereas the high-angle mode is interpreted as a disequilibrium contact angle that forms

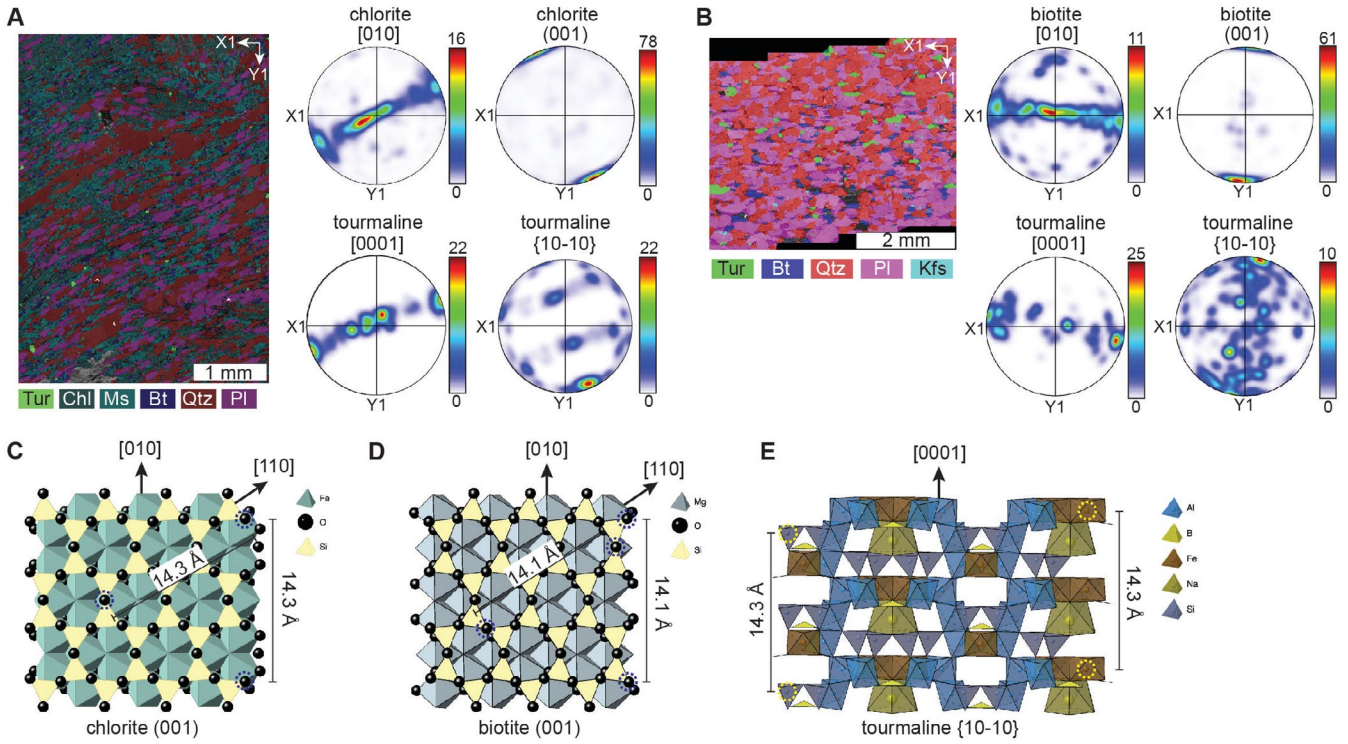

FIGURE 1 | Tourmaline–chlorite and tourmaline–biotite epitaxy. Phase maps and equal-area upper-hemisphere pole figures showing orientations of chlorite and tourmaline from Isua (A) and biotite and tourmaline from Langtang (B). Point-per-pixel pole figures contoured and coloured by multiples of uniform distribution. Epitaxial nucleation of tourmaline is evidenced by the alignment of tourmaline {10–10}[0001] parallel to mica (001)[010]. Tur–tourmaline, Chl–chlorite, Ms–muscovite, Bt–biotite, Qtz–quartz, Pl–plagioclase, Kfs–K-feldspar. Crystal structure and similarity in atomic-spacing of oxygen in chlorite C and biotite D as viewed normal to (001), and Fe, Al, Na, Si in tourmaline E, viewed normal to {10–10}. [Colour figure can be viewed at wileyonlinelibrary.com]

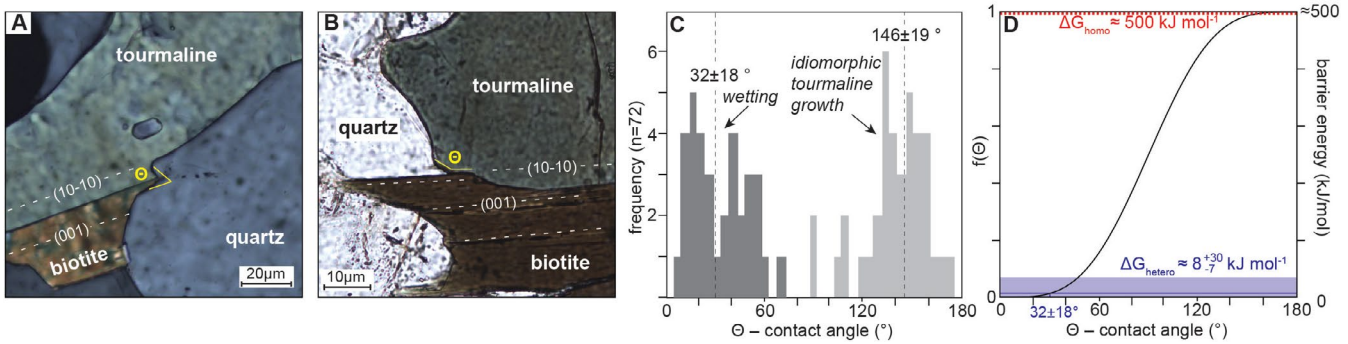

FIGURE 2 | Tourmaline–biotite contact angle. Photomicrograph of tourmaline–biotite (001)–quartz contact angles; due to A wetting (nucleation) and B idiomorphic tourmaline growth (disequilibrium). (C) Frequency distribution of tourmaline–biotite (001)–quartz contact angles. (D) barrier energy as a function of contact angle for homogeneous (red line) and heterogeneous nucleation of tourmaline (i.e., epitaxy; blue line, with a > 92% reduction in nucleation activation energy when compared to that required for homogenous nucleation). [Colour figure can be viewed at wileyonlinelibrary.com]

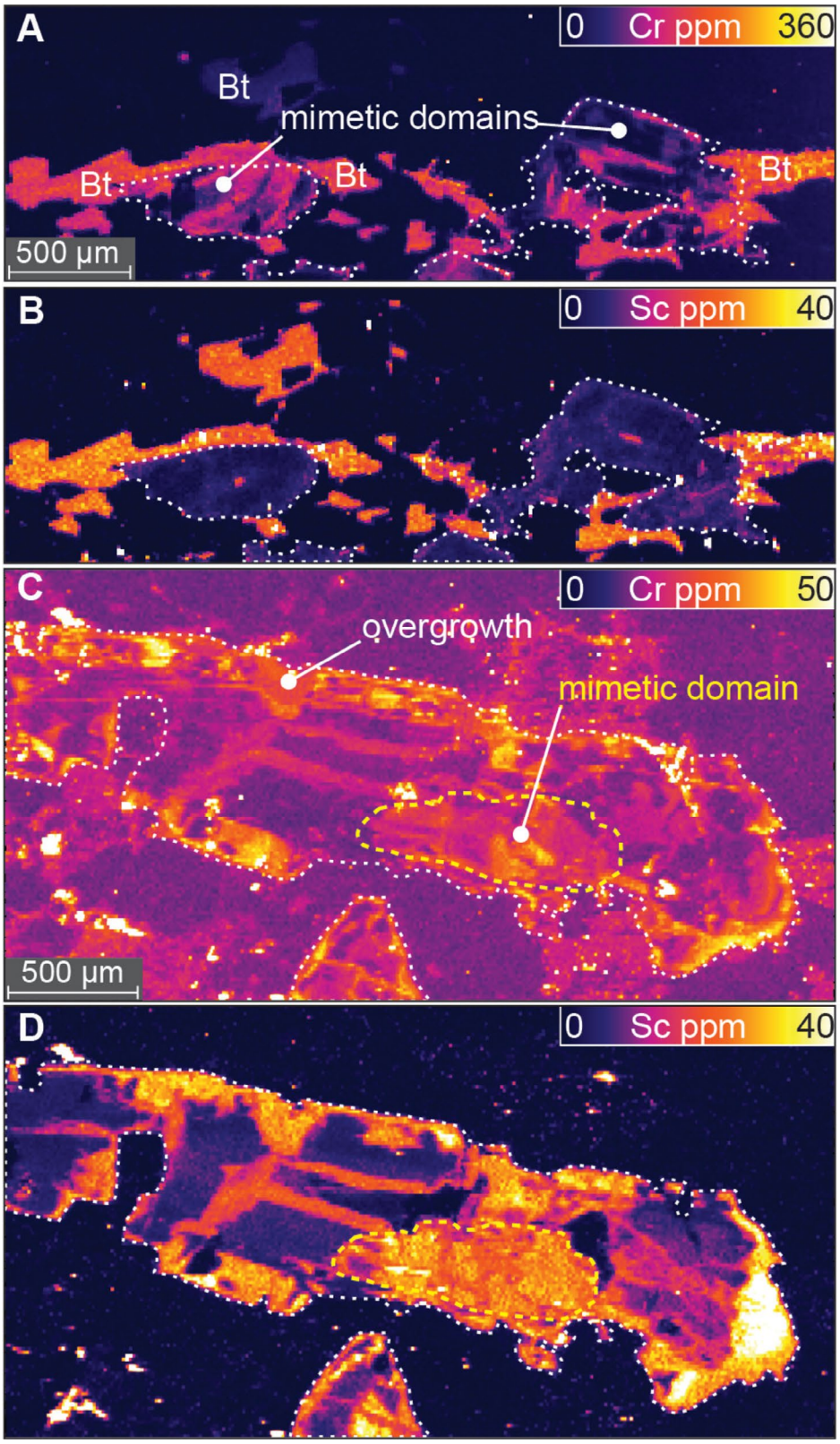

FIGURE 3 | Trace element maps of metamorphic and magmatic tourmaline. LA-ICPMS element concentration maps of metamorphic tourmaline–biotite intergrowths in a Himalayan schist (A, B) and magmatic tourmaline from a Himalayan tourmaline–biotite granite (C, D). Tourmaline grains are outlined by white dashed line. Biotite is the main host phase for Cr and Sc in both samples. Mimetic replacement of biotite by tourmaline incorporates Cr and Sc into tourmaline. [Colour figure can be viewed at wileyonlinelibrary.com]

during the subsequent, idiomorphic tourmaline growth and the stabilization of rational crystal facets (Figure 2B). This low primary contact angle of 32° ± 18° corresponds to a 92%–99% reduction in the activation energy required to nucleate tourmaline epitaxially on biotite when compared to that required for homogeneous nucleation (Figure 2D).

In both orogenic settings and volcanic arcs, a volumetrically minor component of tourmaline forms as a primary magmatic mineral phase (typically < 1 modal %), rather than as a result of reactions with the biotite-rich intrusive margins and host rock (London 1999). Tourmaline bearing granites are typically devoid of biotite, which is consistent with tourmaline forming as a result of reaction with biotite (Wolf and London 1997), with some tourmaline crystals preserving a record of mimetic replacement of biotite in the distribution of trace elements Cr and Sc (Dyck and Larson 2023). Figure 3A,B illustrates an example of mimetic domains found in metamorphic tourmaline that overgrew biotite at the intrusive margin between a granite and a schist, whereas Figure 3C,D shows a similar mimetic domain in the core of a magmatic tourmaline. The mapped distribution of Cr an Sc in the magmatic tourmaline is consistent with the crystal having first nucleating on, and then replacing, pre-existing biotite (Wolf and London 1997). The presence of mimetic cores in granite-hosted tourmaline demonstrates that the same epitaxial nucleation relationship of tourmaline on mica applies to both magmatic and metamorphic crust.

4 | Implications for the Bioavailability of Borate on Rocky Planets

The formation of chemically evolved (granitic) continental crust, emergence of significant subaerial land, and the subsequent, albeit limited, chemical weathering of near surface tourmaline, all contributed to the initiation of the modern-style terrestrial boron cycle. The presence of Hadean zircons early in the geological record (ca. 4400 Ma (Wilde et al. 2001)) attests to early generation of evolved crusts with a continental affinity and the potential to both sequester boron and, upon weathering, release surface-available borate. While the rate at which early continental crust grew remains debated, > 65% of the present volume of continental crust was generated by ca. 3000 Ma (Hawkesworth et al. 2019).

Prior to the formation of a volumetrically significant continental crust on Earth and the attendant stabilization of the peraluminous mica-group minerals biotite and chlorite, the nucleation of tourmaline would have been kinetically unfavourable. Biotite and chlorite are common minerals in peraluminous continental crust. While chlorite is found in hydrated metabasalts, biotite is rare in basaltic oceanic crust. In the absence of appreciable peraluminous continental crust that can stabilize tourmaline, the surface waters of early Earth would have had boron concentrations that are up to three orders of magnitude higher than those on modern-day Earth (Figure 4A). At such elevated boron concentrations, water soluble polyborate ions are stabilized in favour of aqueous borate(s) (Spessard 1970). The emergence of peraluminous continental crust and attendant stabilization of tourmaline acted as a significant sink for Earth's outgassed surface boron, ultimately leading to the stabilization borate(s) in the hydrosphere and modern-day seawater boron concentrations of ~4.4 μg/g (Figure 4B; Marschall 2018).

Given the incompatible nature of boron during mantle melting and its hydrophile nature, it may be expected that any rocky planet undergoing mantle differentiation will similarly concentrate its boron inventory in its surface water. Indeed, any rocky planet that does not express a peraluminous crust on its surface, such as Mars (McSween et al. 2009), is therefore unlikely to possess a crust that sequesters an appreciable amount of boron in the form of tourmaline, leaving instead a hydrosphere enriched in polyborates.

On Earth, the transition from the primary planetary reservoir of boron being aqueous polyborates to that of boron sequestration within mineral hosts has implications for the evolution of life. Unlike borate, which plays a key role in the stabilization of ribose and hence the self-assembly of pre-biotic precursors (Kim et al. 2016; Ricardo et al. 2004), polyborates have no known utilization by life. In experimental prebiotic chemistry, borate minerals stabilize ribose by forming complexes with the sugar's cis-diols, preventing its rapid decomposition in aqueous environments and thereby facilitating the accumulation of ribose necessary for RNA formation (Hirakawa et al. 2022). This stabilization may have been particularly important on the early Earth, where otherwise labile sugars would have degraded before participating in further prebiotic reactions (Ricardo et al. 2004). Thus, the emergence of peraluminous continental crust should be considered a key component in the advent of terrestrial life. Furthermore, as an essential micronutrient for the evolution of higher plants (Bolaños et al. 2004), boron released by near-surface continental weathering should be considered a key component in

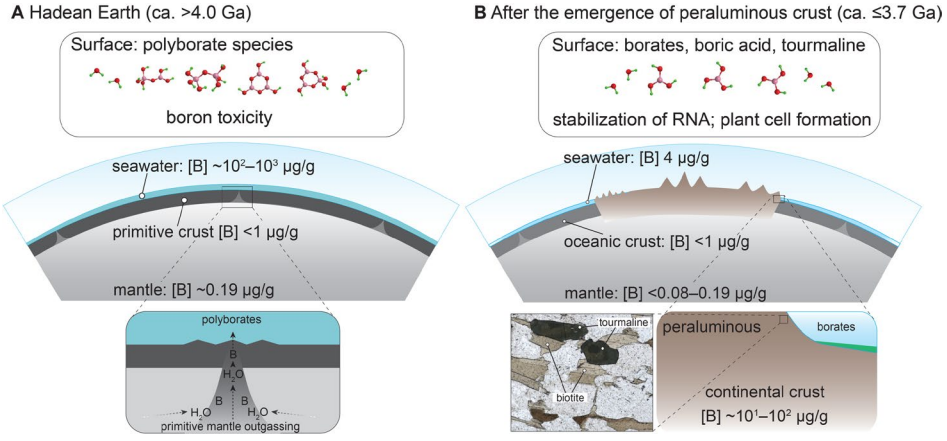

FIGURE 4 | Secular evolution of terrestrial boron reservoirs. Comparison of boron concentrations and speciation for early Earth (A) and after the emergence of peraluminous continental crust (B). [Colour figure can be viewed at wileyonlinelibrary.com]

the colonization of land by plants. In modern plants, boron is required for the structural integrity of cell walls, where it cross-links rhamnogalacturonan II in pectic polysaccharides, thereby maintaining cell wall stability and enabling normal growth and reproductive development (O'Neill et al. 2004). Within the context of higher plant evolution, boron deficiency leads to impaired meristem growth, reduced fertility, and disruption of vascular tissue development (Landi et al. 2019; Nable et al. 1997). Beyond plants, boron also participates in a small number of microbial metabolic systems, including quorum-sensing molecules such as autoinducer-2 borate complexes that mediate interspecies communication in bacteria (Chen et al. 2002). Because of the emergence of peraluminous continental crust and resulting tourmaline-mica epitaxy, the largely subaerial continental environments where borates are found today have likely long remained a crucial reservoir of bioavailable boron and may have provided a vital fertilizer for terrestrial life.

Acknowledgements

We thank editor Carlo Doglioni two anonymous reviewers for suggestions that improved this manuscript. We also thank Dr. Claire Nichols for providing access to the Isua sample and Dr. Mark Button for assistance in processing LA-ICPMS data.

Funding

Natural Sciences and Engineering Research Council of Canada grant R611772 (Brendan V. Dyck) Canadian Foundation for Innovation 42967 (Brendan V. Dyck).

Conflicts of Interest

The authors declare no conflicts of interest.

Data Availability Statement

All EBSD data (.ctf format) used in this article are available in the Supporting Information file and stored in the Open Science Framework online repository at: https://osf.io/ufk7p/?view_only=dac9f3eb76fc486bb72b658fcc58eaca.

References

Ballentine, C. J., and G. Holland. 2008. "What CO_2 Well Gases Tell Us About the Origin of Noble Gases in the Mantle and Their Relationship to the Atmosphere." *Philosophical Transactions of the Royal Society A: Mathematical, Physical and Engineering Sciences* 366, no. 1883: 4183–4203. https://doi.org/10.1098/rsta.2008.0150.

Bolaños, L., K. Lukaszewski, I. Bonilla, and D. Blevins. 2004. "Why Boron?" *Plant Physiology and Biochemistry* 42, no. 11: 907–912.

Byerly, G. R., and M. R. Palmer. 1991. "Tourmaline Mineralization in the Barberton Greenstone Belt, South Africa: Early Archean Metasomatism by Evaporite-Derived Boron." *Contributions to Mineralogy and Petrology* 107, no. 3: 387–402. https://doi.org/10.1007/BF00325106.

Chaussidon, M., and A. Jambon. 1994. "Boron Content and Isotopic Composition of Oceanic Basalts: Geochemical and Cosmochemical Implications." *Earth and Planetary Science Letters* 121, no. 3-4: 277–291.

Chen, X., S. Schauder, N. Potier, et al. 2002. "Structural Identification of a Bacterial Quorum-Sensing Signal Containing Boron." *Nature* 415, no. 6871: 545–549.

Donald, I. W. 1995. "The Crystallization Kinetics of a Glass Based on the Cordierite Composition Studied by DTA and DSC." *Journal of Materials Science* 30, no. 4: 904–915. https://doi.org/10.1007/BF01178424.

Dyck, B., and K. P. Larson. 2023. "Metasomatic Origin of the Himalayan Banded Tourmaline Leucogranite." *Contributions to Mineralogy and Petrology* 178, no. 7: 37. https://doi.org/10.1007/s00410-023-02020-0.

Garrett, D. E. 1996. *Borate Minerals and the Origin of Borate Deposits*. Elsevier. https://www.sciencedirect.com/book/9780122760600/borates.

Grew, E. S. 2017. "Boron: From Cosmic Scarcity to 300 Minerals." *Elements: An International Magazine of Mineralogy, Geochemistry, and Petrology* 13, no. 4: 225–229.

Grew, E. S., R. F. Dymek, J. C. De Hoog, et al. 2015. "Boron Isotopes in Tourmaline From the Ca. 3.7–3.8 Ga Isua Supracrustal Belt, Greenland: Sources for Boron in Eoarchean Continental Crust and Seawater." *Geochimica et Cosmochimica Acta* 163: 156–177.

Hawkesworth, C., P. A. Cawood, and B. Dhuime. 2019. "Rates of Generation and Growth of the Continental Crust." *Geoscience Frontiers* 10, no. 1: 165–173.

Henry, D. J., and B. L. Dutrow. 1996. "Chapter 10. Metamorphic Tourmaline and Its Petrologic Applications." In *Boron*, edited by L. M. Anovitz and E. S. Grew, 503–558. De Gruyter. https://doi.org/10.1515/9781501509223-012.

Henry, D. J., M. Novák, F. C. Hawthorne, et al. 2011. "Nomenclature of the Tourmaline-Supergroup Minerals." *American Mineralogist* 96, no. 5–6: 895–913.

Hirakawa, Y., T. Kakegawa, and Y. Furukawa. 2022. "Borate-Guided Ribose Phosphorylation for Prebiotic Nucleotide Synthesis." *Scientific Reports* 12, no. 1: 11828.

Kelton, K. F. 2001. "Nucleation." In *Encyclopedia of Materials: Science and Technology*, 6388–6392. Springer.

Kim, H., Y. Furukawa, T. Kakegawa, A. Bita, R. Scorei, and S. A. Benner. 2016. "Evaporite Borate-Containing Mineral Ensembles Make Phosphate Available and Regiospecifically Phosphorylate Ribonucleosides: Borate as a Multifaceted Problem Solver in Prebiotic Chemistry." *Angewandte Chemie* 128, no. 51: 16048–16052. https://doi.org/10.1002/ange.201608001.

Landi, M., T. Margaritopoulou, I. E. Papadakis, and F. Araniti. 2019. "Boron Toxicity in Higher Plants: An Update." *Planta* 250, no. 4: 1011–1032. https://doi.org/10.1007/s00425-019-03220-4.

Leeman, W. P., and V. B. Sisson. 1996. "Chapter 12. Geochemistry of Boron and Its Implications for Crustal and Mantle Processes." In *Boron*, edited by L. M. Anovitz and E. S. Grew, 645–708. De Gruyter. https://doi.org/10.1515/9781501509223-014.

London, D. 1999. "Stability of Tourmaline in Pei Aluminous Granite Systems: The Boron Cycle From Anatexis to Hydrothermal Aureoles." *European Journal of Mineralogy* 11: 253–262.

London, D. 2011. "Experimental Synthesis and Stability of Tourmaline: A Historical Overview." *Canadian Mineralogist* 49, no. 1: 117–136.

Markov, I., and S. Stoyanov. 1987. "Mechanisms of Epitaxial Growth." *Contemporary Physics* 28, no. 3: 267–320. https://doi.org/10.1080/00107518708219073.

Marschall, H. R. 2018. "Boron Isotopes in the Ocean Floor Realm and the Mantle." In *Boron Isotopes*, edited by H. Marschall and G. Foster, 189–215. Springer International Publishing. https://doi.org/10.1007/978-3-319-64666-4_8.

Marschall, H. R., V. D. Wanless, N. Shimizu, P. A. E. Pogge von Strandmann, T. Elliott, and B. D. Monteleone. 2017. "The Boron and Lithium Isotopic Composition of Mid-Ocean Ridge Basalts and the

Mantle." *Geochimica et Cosmochimica Acta* 207: 102–138. https://doi.org/10.1016/j.gca.2017.03.028.

McSween, H. Y., G. J. Taylor, and M. B. Wyatt. 2009. "Elemental Composition of the Martian Crust." *Science* 324, no. 5928: 736–739. https://doi.org/10.1126/science.1165871.

Nable, R. O., G. S. Bañuelos, and J. G. Paull. 1997. "Boron Toxicity." *Plant and Soil* 193, no. 1–2: 181–198. https://doi.org/10.1023/A:1004272227886.

O'Neill, M. A., T. Ishii, P. Albersheim, and A. G. Darvill. 2004. "Rhamnogalacturonan II: Structure and Function of a Borate Cross-Linked Cell Wall Pectic Polysaccharide." *Annual Review of Plant Biology* 55, no. 1: 109–139. https://doi.org/10.1146/annurev.arplant.55.031903.141750.

Palin, R. M., and B. Dyck. 2021. "Metamorphism of Pelitic (Al-Rich) Rocks." *Encyclopedia of Geology* 2: 445–456.

Ricardo, A., M. A. Carrigan, A. N. Olcott, and S. A. Benner. 2004. "Borate Minerals Stabilize Ribose." *Science* 303, no. 5655: 196. https://doi.org/10.1126/science.1092464.

Rubey, W. W. 1951. "Geologic History of Sea Water: An Attempt to State the Problem." *Geological Society of America Bulletin* 62, no. 9: 1111–1148.

Rudnick, R. L., and S. Gao. 2003. "Composition of the Continental Crust." In *Treatise on Geochemistry*, 1–64. Elsevier. https://doi.org/10.1016/B0-08-043751-6/03016-4.

Scaillet, B., M. Pichavant, and J. Roux. 1995. "Experimental Crystallization of Leucogranite Magmas." *Journal of Petrology* 36, no. 3: 663–705.

Schilling, J., C. K. Unni, and M. L. Bender. 1978. "Origin of Chlorine and Bromine in the Oceans." *Nature* 273, no. 5664: 631–636.

Spessard, J. E. 1970. "Investigations of Borate Equilibria in Neutral Salt Solutions." *Journal of Inorganic and Nuclear Chemistry* 32, no. 8: 2607–2613.

Sun, S., and W. F. McDonough. 1989. "Chemical and Isotopic Systematics of Oceanic Basalts: Implications for Mantle Composition and Processes." *Geological Society, London, Special Publications* 42, no. 1: 313–345. https://doi.org/10.1144/GSL.SP.1989.042.01.19.

Thomas, R. W., J. Wade, and B. J. Wood. 2023. "The Bonding Environment of Chlorine in Silicate Melts." *Chemical Geology* 617: 121269.

Touret, J. L. R., M. Santosh, and J. M. Huizenga. 2022. "Composition and Evolution of the Continental Crust: Retrospect and Prospect." *Geoscience Frontiers* 13, no. 5: 101428.

Van Hinsberg, V. J., D. J. Henry, and H. R. Marschall. 2011. "Tourmaline: An Ideal Indicator of Its Host Environment." *Canadian Mineralogist* 49, no. 1: 1–16.

Vorbach, A. 1989. "Experimental Examinations on the Stability of Synthetic Tourmalines in Temperatures From 250 Degree C to 750 Degree C and Pressures up to 4 Kb." *Neues Jahrbuch für Mineralogie (Abhandlungen)* 161, no. 1: 69–83.

Wedepohl, K. H. 1995. "The Composition of the Continental Crust." *Geochimica et Cosmochimica Acta* 59, no. 7: 1217–1232.

Wilde, S. A., J. W. Valley, W. H. Peck, and C. M. Graham. 2001. "Evidence From Detrital Zircons for the Existence of Continental Crust and Oceans on the Earth 4.4 Gyr Ago." *Nature* 409, no. 6817: 175–178.

Wolf, M. B., and D. London. 1997. "Boron in Granitic Magmas: Stability of Tourmaline in Equilibrium With Biotite and Cordierite." *Contributions to Mineralogy and Petrology* 130, no. 1: 12–30. https://doi.org/10.1007/s004100050346.

Wood, B. J., D. J. Smythe, and T. Harrison. 2019. "The Condensation Temperatures of the Elements: A Reappraisal." *American Mineralogist* 104, no. 6: 844–856. https://doi.org/10.2138/am-2019-6852CCBY.

You, C.-F., A. J. Spivack, J. H. Smith, and J. M. Gieskes. 1993. "Mobilization of Boron in Convergent Margins: Implications for the Boron Geochemical Cycle." *Geology* 21, no. 3: 207–210.

Yuan, L., and G. Steinle-Neumann. 2022. "Possible Control of Earth's Boron Budget by Metallic Iron." *Geophysical Research Letters* 49, no. 10: e2021GL096923. https://doi.org/10.1029/2021GL096923.

Supporting Information

Additional supporting information can be found online in the Supporting Information section. **Figure S1:** Electron backscatter diffraction phase map and equal-area upper-hemisphere pole figures showing point-per-pixel orientations of tourmaline and biotite from the Himalayan psammitic biotite–tourmaline schist. Pole figures are contoured and coloured by multiples of uniform distribution. **Figure S2:** Electron backscatter diffraction phase map and contoured equal-area upper-hemisphere pole figures showing point-per-pixel orientations of tourmaline (schorl endmember) and chlorite (clinochlore endmember) from the Isua pelitic garnet–staurolite–tourmaline schist. Pole figures are contoured and coloured by multiples of uniform distribution. **Table S1:** Measurements of tourmaline–biotite (001)–quartz dihedral angles in Langtang sample (BD1432), made using a 4-axis universal stage.